SANTA CRUZ BIOTECHNOLOGY, INC.

AQP2 (E-2): sc-515770

SANTA CRUZ BIOTECHNOLOGY

The Power to Question

BACKGROUND

Aquaporins (AQPs) are a large family of integral membrane water transport channel proteins that facilitate the transport of water through the cell membrane. This function is conserved in animals, plants and bacteria. Many isoforms of aquaporin have been identified in mammals, designated AQP0 through AQP10. Aquaporins are widely distributed and it is not uncommon for more than one type of AQP to be present in the same cell. Although most aquaporins are only permeable to water, AQP3, AQP7 and AQP9 and one of the two AQP10 transcripts are also permeable to urea and glycerol. AQP2 is the only water channel that is activated by vasopressin to enhance water reabsorption in the kidney collecting duct. Aquaporins are involved in renal water absorption, generation of pulmonary secretions, lacrimation, and the secretion and reabsorption of cerebrospinal fluid and aqueous humor.

CHROMOSOMAL LOCATION

Genetic locus: AQP2 (human) mapping to 12q13.12; Aqp2 (mouse) mapping to 15 F1.

SOURCE

AQP2 (E-2) is a mouse monoclonal antibody raised against amino acids 232-271 mapping within a C-terminal cytoplasmic domain of AQP2 of human origin.

PRODUCT

Each vial contains 200 µg IgG_1 kappa light chain in 1.0 ml of PBS with < 0.1% sodium azide and 0.1% gelatin.

AQP2 (E-2) is available conjugated to agarose (sc-515770 AC), 500 µg/0.25 ml agarose in 1 ml, for IP; to HRP (sc-515770 HRP), 200 µg/ml, for WB, IHC(P) and ELISA; to either phycoerythrin (sc-515770 PE), fluorescein (sc-515770 FITC), Alexa Fluor® 488 (sc-515770 AF488), Alexa Fluor® 546 (sc-515770 AF546), Alexa Fluor® 594 (sc-515770 AF594) or Alexa Fluor® 647 (sc-515770 AF647), 200 µg/ml, for WB (RGB), IF, IHC(P) and FCM; and to either Alexa Fluor® 680 (sc-515770 AF680) or Alexa Fluor® 790 (sc-515770 AF790), 200 µg/ml, for Near-Infrared (NIR) WB, IF and FCM.

Alexa Fluor® is a trademark of Molecular Probes, Inc., Oregon, USA

APPLICATIONS

AQP2 (E-2) is recommended for detection of AQP2 of mouse, rat and human origin by Western Blotting (starting dilution 1:100, dilution range 1:100-1:1000), immunoprecipitation [1-2 µg per 100-500 µg of total protein (1 ml of cell lysate)], immunofluorescence (starting dilution 1:50, dilution range 1:50-1:500), immunohistochemistry (including paraffin-embedded sections) (starting dilution 1:50, dilution range 1:50-1:500) and solid phase ELISA (starting dilution 1:30, dilution range 1:30-1:3000).

Suitable for use as control antibody for AQP2 siRNA (h): sc-42363, AQP2 siRNA (m): sc-42364, AQP2 shRNA Plasmid (h): sc-42363-SH, AQP2 shRNA Plasmid (m): sc-42364-SH, AQP2 shRNA (h) Lentiviral Particles: sc-42363-V and AQP2 shRNA (m) Lentiviral Particles: sc-42364-V.

Molecular Weight of unglycosylated AQP2: 29 kDa.

Molecular Weight of mature AQP2: 35-45 kDa.

STORAGE

Store at 4° C, **DO NOT FREEZE**. Stable for one year from the date of shipment. Non-hazardous. No MSDS required.

DATA

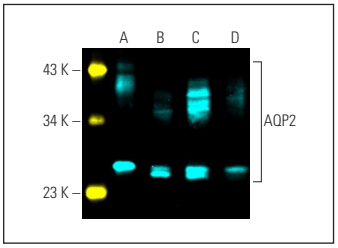

AQP2 (E-2) Alexa Fluor® 647: sc-515770 AF647. Direct fluorescent western blot analysis of AQP2 expression in human kidney (**A**), mouse postnatal kidney (**B**), mouse kidney (**C**) and rat kidney (**D**) tissue extracts. Blocked with UltraCruz® Blocking Reagent: sc-516214. Cruz Marker™ Molecular Weight Standards detected with Cruz Marker™ MW Tag-Alexa Fluor® 488: sc-516790.

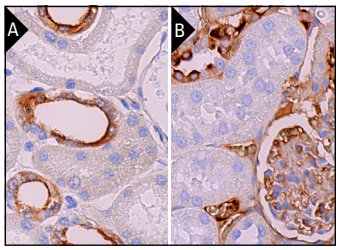

AQP2 (E-2): sc-515770. Immunoperoxidase staining of formalin fixed, paraffin-embedded human kidney tissue showing membrane and cytoplasmic staining of cells in tubules (**A**). Immunoperoxidase staining of formalin fixed, paraffin-embedded rat kidney tissue showing membrane and cytoplasmic staining of cells in glomeruli and cells in tubules (**B**).

SELECT PRODUCT CITATIONS

1. Pizzoni, A., et al. 2018. AQP2 can modulate the pattern of Ca^{2+} transients induced by store-operated Ca^{2+} entry under TRPV4 activation. J. Cell. Biochem. 119: 4120-4133.
2. Hu, S., et al. 2019. Inhibition of IL-1β by aliskiren improved renal AQP2 expression and urinary concentration defect in ureteral obstruction and release. Front. Physiol. 10: 1157.
3. Albertoni Borghese, M.F., et al. 2020. Inhibition of endothelin system during the postnatal nephrogenic period in the rat. Its relationship with hypertension and renal disease in adulthood. PLoS ONE 15: e0229756.
4. Machiguchi, T. and Nakamura, T. 2020. Regenerated nephrons in kidney cortices ameliorate exacerbated serum creatinine levels in rats with adriamycin nephropathy. Biochem. Biophys. Res. Commun. 530: 541-546.
5. Mae, S.I., et al. 2020. Expansion of human iPSC-derived ureteric bud organoids with repeated branching potential. Cell Rep. 32: 107963.
6. Tahaei, E., et al. 2020. Distal convoluted tubule sexual dimorphism revealed by advanced 3D-imaging. Am. J. Physiol. Renal Physiol. 319: F754-F764.
7. Chen, Q.G., et al. 2020. Optimization of urinary small extracellular vesicle isolation protocols: implications in early diagnosis, stratification, treatment and prognosis of diseases in the era of personalized medicine. Am. J. Transl. Res. 12: 6302-6313.
8. Schumann, A., et al. 2021. Defective lysosomal storage in Fabry disease modifies mitochondrial structure, metabolism and turnover in renal epithelial cells. J. Inherit. Metab. Dis. 44: 1039-1050.

RESEARCH USE

For research use only, not for use in diagnostic procedures.